Electronic Supplementary Material (ESI) for Reaction Chemistry & Engineering.
This journal is © The Royal Society of Chemistry 2022

Supporting Information for

Experimental insights on catalytic oxidation of 1,6-hexanediol to ε-caprolactone over (*p*-cymene)$RuCl_2$(L) complexes in non-polar media

Pratya Promchana,[a] Kittisak Choojun,*[a,b] Nararak Leesakul,[c] Saowanit Saithong,[c] Kittipong Chainok,[d] and Tawan Sooknoi **[a,b]

[a] Department of Chemistry, School of Science, King Mongkut's Institute of Technology Ladkrabang, Chalongkrung Road, Ladkrabang, Bangkok, 10520, Thailand

[b] Catalytic Chemistry Research Unit, School of Science, King Mongkut's Institute of Technology Ladkrabang, Chalongkrung Road, Ladkrabang, Bangkok, 10520, Thailand

[c] Division of Physical Science and Center of Excellence for Innovation in Chemistry, Faculty of Science, Prince of Songkla University, Hat-Yai, Songkhla, 90112, Thailand

[d] Materials and Textile Technology, Faculty of Science and Technology, Thammasat University, Klong Luang, Pathum Thani, 12121 Thailand

Crystallographic details of the new (*p*-cymene)$RuCl_2(L_{N3})$ compound

For the new (*p*-cymene)$RuCl_2(L_{N3})$ complex, the reaction was performed in dichloromethane at room temperature. This complex is air-stable under ambient conditions, and its structure is confirmed by NMR spectra, as shown in Figures S1-S2. These complexes are soluble in common organic solvents, such as acetone, DMF, CH_2Cl_2, and methanol. However, they are insoluble in water.

The crystallographic details and molecular structure of a new (*p*-cymene)$RuCl_2(L_{N3})$ complex are shown in Table S1 and Figure S3, respectively. The selected bond lengths and angles are summarized in Table S2. It can be seen that this complex has a pseudo-tetrahedral geometry with vertex distances of 2.408(10), 2.418(9), 2.129(3), and 1.669 Å for Ru-Cl(1), Ru-Cl(2), Ru-N, and Ru-(centroid of the *p*-cymene ring), respectively. While, the bond length of Ru-C (in *p*-cymene) is in the range of 2.174(6)-2.204(0) Å, which is similar to those reported in the literature.[1-7] In this complex, the Ru-N is slightly shorter than those of (*p*-cymene)$RuCl_2(L_{N1})$ (2.17 Å).[5] This could attribute to the higher electron density of 4-*tert*-butylpyridine (L_{N3}) as compared to pyridine (L_{N1}). Accordingly, a stronger overlapping interaction between Ru and alkyl-substituted ligands could be expected. In a supportive manner, the previously reported complexes with a donating group on pyridine ligand (i.e., L_{N2} and L_{N5}) also show a shorter Ru-N bond (~2.13 Å) (Table S2, entry 3).[6-7]

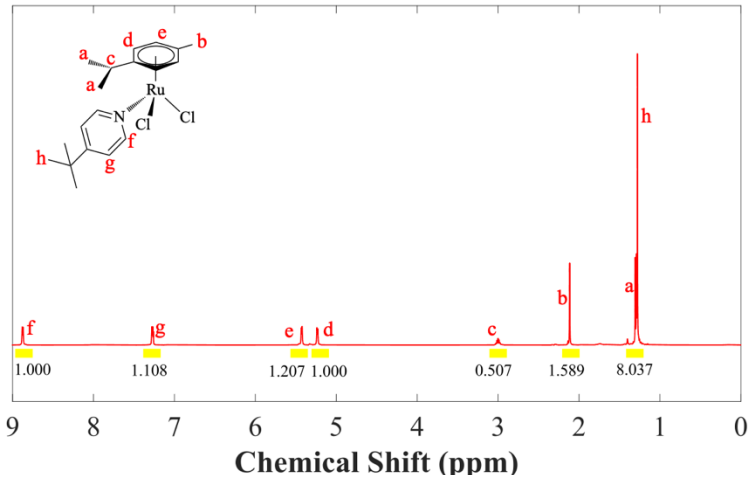

Figure S1. ^{1}H 500 MHz NMR spectrum of (*p*-cymene)$RuCl_2(L_{N3})$ in chloroform-d_1.

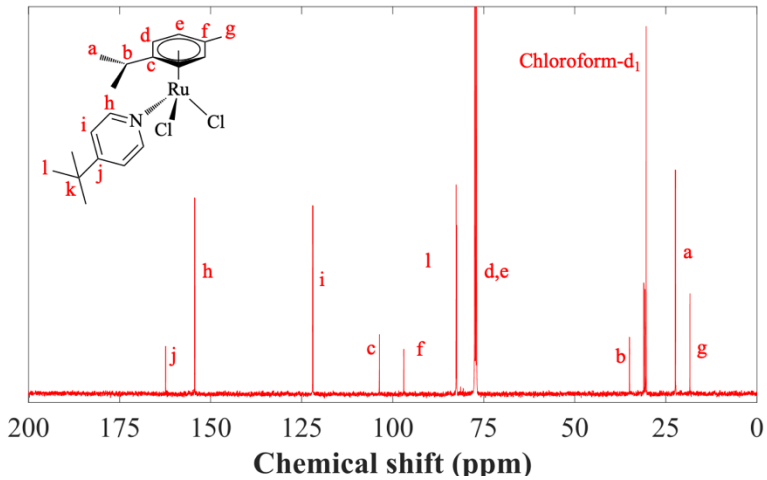

Figure S2. ^{13}C 500 MHz NMR spectrum of (*p*-cymene)$RuCl_2(L_{N3})$ in chloroform-d_1.

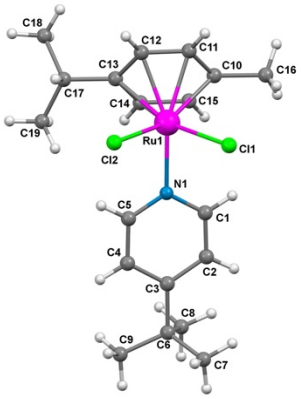

Figure S3. ORTEP representation (50% probability ellipsoid) of complex (*p*-cymene)$RuCl_2(L_{N3})$ (minor disorder part of the methyl group at C6 are omitted for clarity).

Table S1. Crystallographic detail of (*p*-cymene)$RuCl_2(L_{N3})$.

Compound complex	**(*p*-cymene)$RuCl_2$(4-*tert*-butylpyridine)**
Formula	$C_{19}H_{27}RuNCl_2$
Formula weight	441.38
Temperature	296(2) K
Wavelength	0.71073 Å
Crystal system	Monoclinic
Space group	*C*2/*c*
Unit cell dimensions	a = 22.7883(10) Å b = 14.3449(6) Å β = 111.2710(10)˚ c = 12.9580(6) Å
Volume	3947.3 $Å^3$
Density (calculated)	1.485 Mg m^{-3}
Absorption coefficient	1.064 mm^{-1}
F(000)	1808
Crystal size	0.400 x 0.120 x 0.120 mm^3
Theta range for data collection	5-50˚ 3.103 to 24.997˚
Index ranges	-27<=h<=27, -16<=k<=17, -15<=l<=15
Reflections collected	47536
Independent reflections	3772 [R(int) =0.0849]
Completeness to theta max = 24.997˚	99.9%
Refinement method	Full-matrix least-squares on F^2
Data/restraints/parameters	3772 / 102 / 245
Goodness-of-fit on F^2	1.040
Final R indices	R1 = 0.0353, wR2 = 0.0758
R indices (all data)	R1 = 0.0519, wR2 = 0.0830
Largest diff. peak and hole	0.888 and -0.735 e.$Å^{-3}$
CCDC Number	1970821

Table S2. Selected bond distances (Å) and bond angles (˚) for the Ru complexes.

Entry	Atom	(*p*-cymene)$RuCl_2$(L)							
		L_{P1}[1]	L_{P2}[2]	L_{P4}[3]	L_{P5}[4]	L_{N1}[5]	L_{N2}[6]	L_{N3}	L_{N5}[7]
		Distances (Å)							
1	Ru-Cl(1)	2.402(3)	2.3992(8)	2.4151(5)	2.4039(9)	2.4515(5)	2.423(2)	2.4082(10)	2.414(2)
2	Ru-Cl(2)	2.379(4)	2.4022(8)	2.4154(6)	2.415(1)	2.4382(5)	2.426(2)	2.4178(9)	2.409(2)
3	Ru-L	2.425(2)	2.2642(8)	2.3438(6)	2.3500(8)	2.172(1)	2.133(6)	2.1290(3)	2.124(8)
4	Ru-(centroid of *p*-cymene)	1.705	1.701	1.708	1.694	1.686	1.677	1.6690	1.658
5	Ru-C(10)	2.225	2.223	2.213	2.203	2.220	2.214	2.201(4)	2.184
6	Ru-C(11)	2.212	2.203	2.176	2.161	2.212	2.183	2.187(4)	2.166
7	Ru-C(12)	2.219	2.178	2.213	2.178	2.229	2.178	2.174(4)	2.192
8	Ru-C(13)	2.218	2.199	2.247	2.205	2.246	2.225	2.197(4)	2.193
9	Ru-C(14)	2.225	2.242	2.245	2.235	2.215	2.179	2.174(3)	2.168
10	Ru-C(15)	2.195	2.247	2.216	2.226	2.189	2.182	2.177(3)	2.153
11	Average Ru-Cl	2.391	2.401	2.415	2.409	2.445	2.425	2.413	2.412
		Angles (˚)							
12	Cl(1)-Ru-Cl(2)	88.0(1)	87.45(2)	88.40(2)	88.78(3)	87.45(1)	88.87(6)	87.94(4)	88.73(7)
13	Cl(1)-Ru-L	87.5(1)	85.02(2)	90.27(2)	82.45(3)	85.88(4)	84.8(2)	84.36(8)	87.0(2)
14	Cl(2)-Ru-L	87.4(1)	87.91(3)	87.10(2)	87.85(3)	86.85(4)	85.5(2)	87.52(8)	85.86(2)
15	C(1)-N-C(5)	-	-	-	-	118.0(2)	118.3(6)	116.60(3)	115.1(6)
16	X(1)-P-X(2)	106.4(5)	102.0(1)	100.81(9)	103.2(2)	-	-	-	-
17	X(1)-P-X(3)	101.0(5)	104.7(1)	106.29(9)	105.1(2)	-	-	-	-
18	X(2)-P-X(3)	101.8(4)	98.7(1)	99.56(9)	105.4(2)	-	-	-	-
19	Cl(1)-Ru-(centroid *p*-cymene)	124.36	126.86	124.67	124.76	128.90	127.26	127.80(6)	125.76
20	Cl(2)-Ru-(centroid *p*-cymene)	123.84	123.97	125.86	127.13	128.78	128.96	127.37(7)	128.55
21	L(1)-Ru-(centroid *p*-cymene)	132.31	131.61	128.20	131.56	128.94	128.16	127.68(9)	127.53

L represents coordinated P, or N X represents ligand substituent C or O

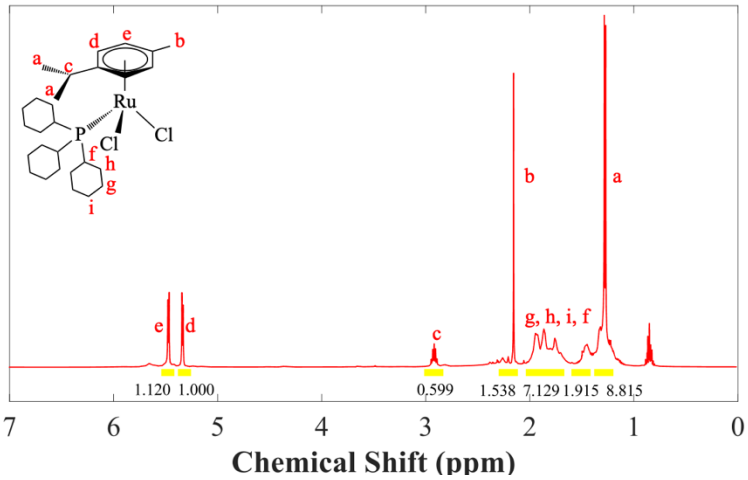

Figure S4. ^{1}H 500 MHz NMR spectrum of (*p*-cymene)$RuCl_2(L_{P1})$ in chloroform-d_1.

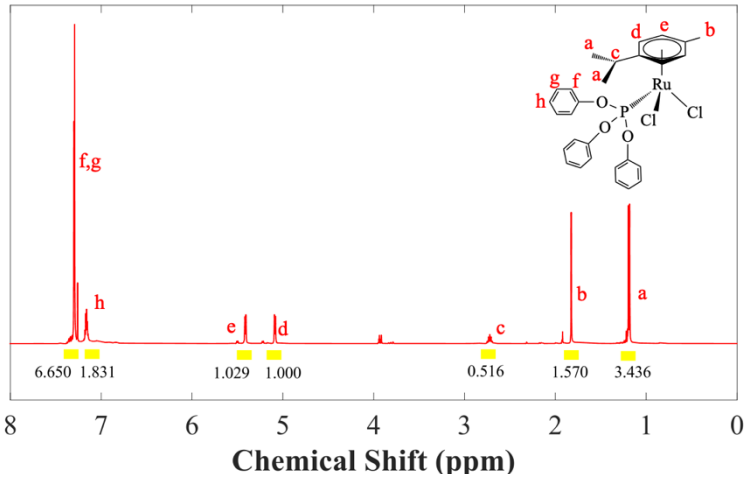

Figure S5. ^{1}H 500 MHz NMR spectrum of (*p*-cymene)$RuCl_2(L_{P2})$ in chloroform-d_1.

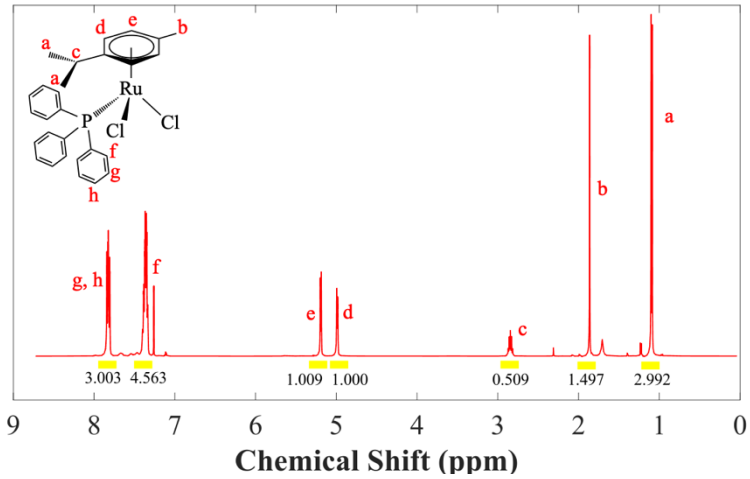

Figure S6. ^{1}H 500 MHz NMR spectrum of (*p*-cymene)$RuCl_2(L_{P4})$ in chloroform-d_1.

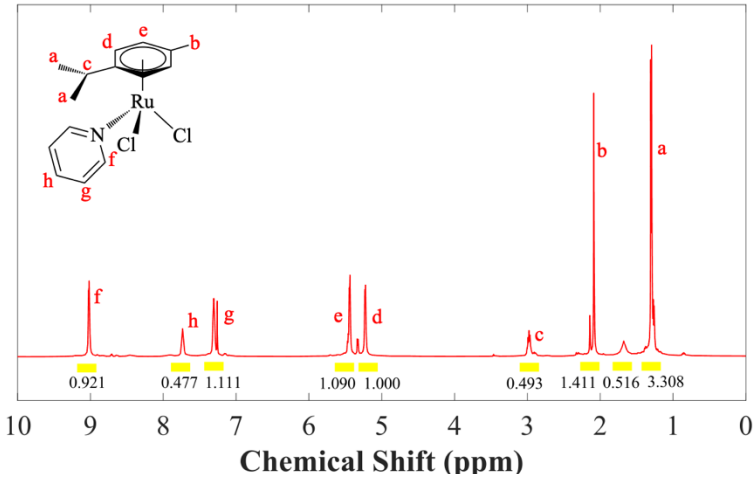

Figure S7. ^{1}H 500 MHz NMR spectrum of (*p*-cymene)$RuCl_2(L_{N1})$ in chloroform-d_1.

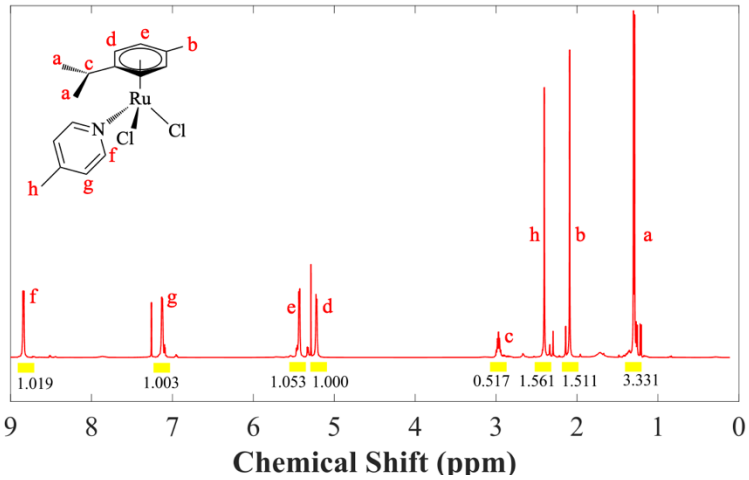

Figure S8. ^{1}H 500 MHz NMR spectrum of (*p*-cymene)$RuCl_2(L_{N2})$ in chloroform-d_1.

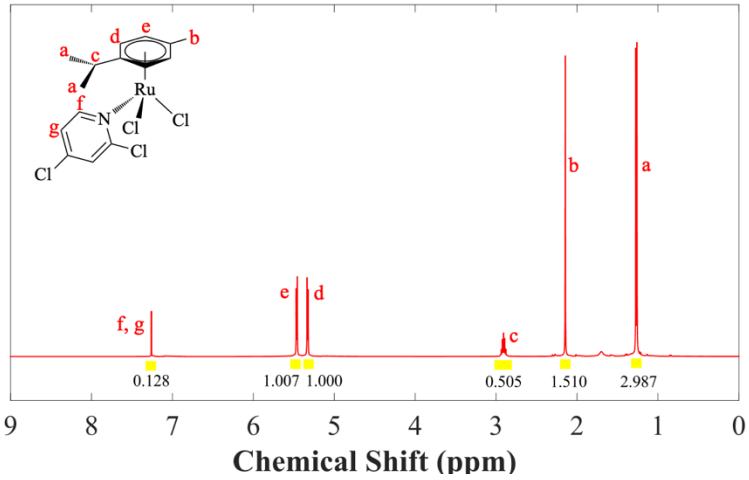

Figure S9. ^{1}H 500 MHz NMR spectrum of (*p*-cymene)$RuCl_2(L_{N4})$ in chloroform-d_1.

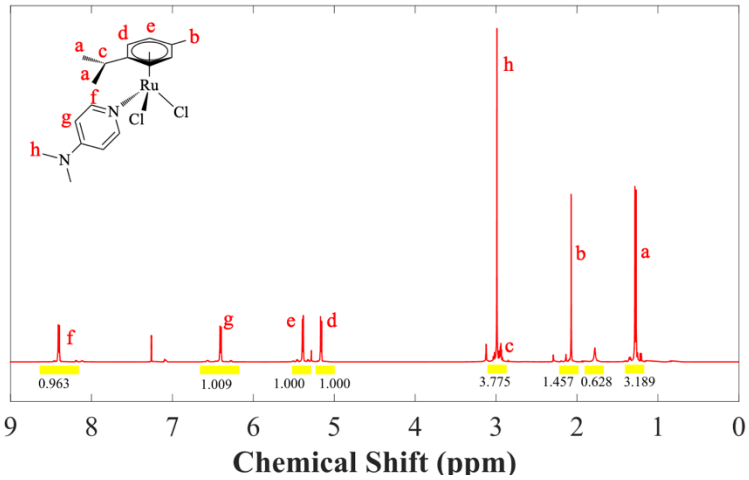

Figure S10. ^{1}H 500 MHz NMR spectrum of (*p*-cymene)$RuCl_2(L_{N5})$ in chloroform-d_1.

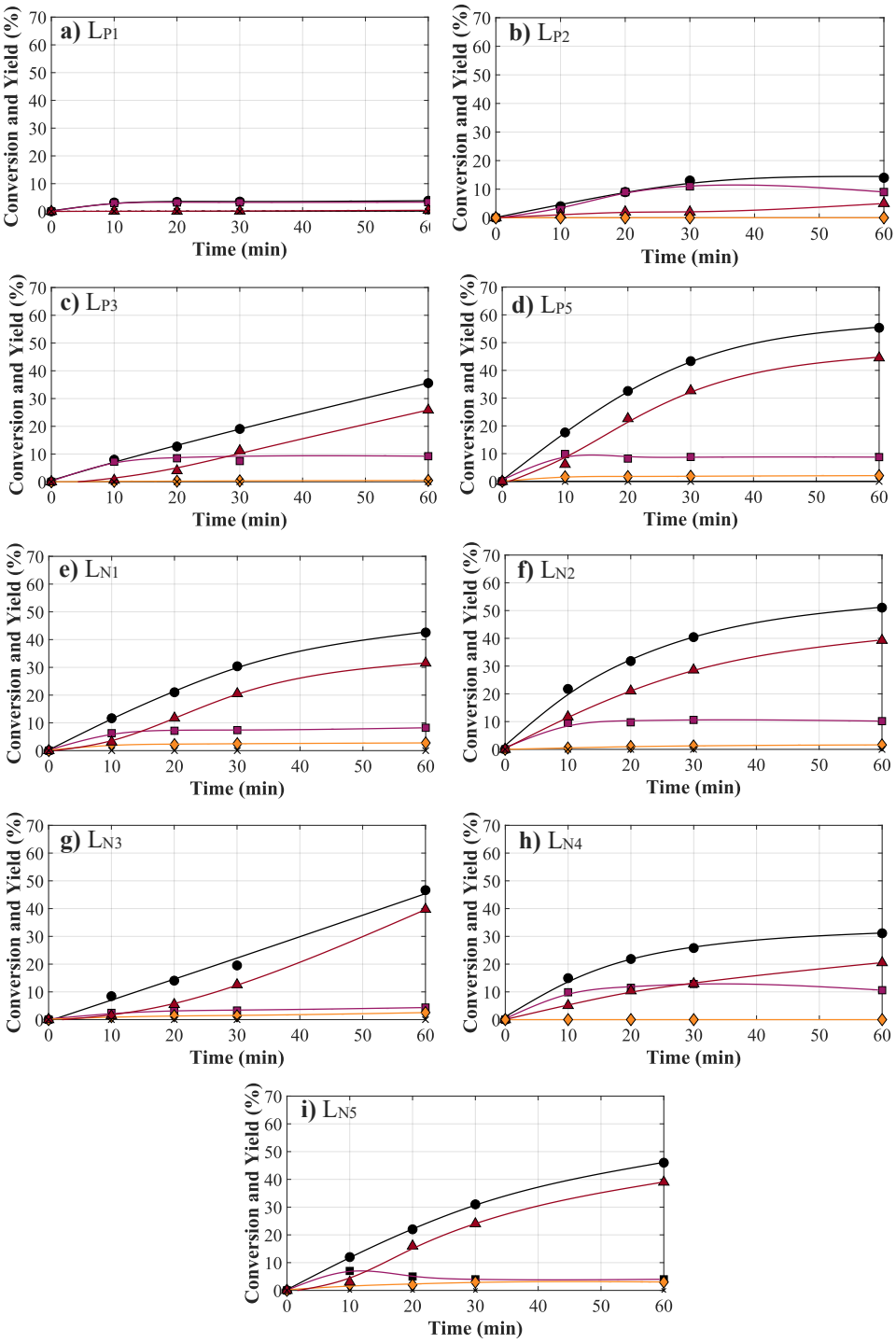

Figure S11. 1,6-HD oxidation time profile using (*p*-cymene)$RuCl_2L$ catalysts where a) L_{P1}, b) L_{P2}, c) L_{P3}, d) L_{P5}, e) L_{N1}, f) L_{N2} g) L_{N3}, h) L_{N4}, i) L_{N5} and j) [(*p*-cymene)$RuCl_2$]$_2$ catalyst (conversion (●), 6-hydroxyhexa-1-nal (■), 1,6-hexanedial (♦), ε-CL (▲), and adipic acid (✕) (0.025 mmol Ru complex, 1 mmol 1,6-HD, under N_2 atmosphere, 110 °C, 30 mL toluene, 0.2 mmol K_2CO_3, 8 mmol MIBK).

Table S3. 6-Hydroxyhexan-1-al and ε-caprolactone selectivity at the similar conversion extrapolated from the reaction profile using (*p*-cymene)$RuCl_2$(L) catalysts.

Entry	Ligands	Bases	Conversion (%)	Selectivity (%)	
				6-Hydroxyhexan-1-al	ε-CL
1	L_{P3}	K_2CO_3	28	36	64
2	L_{P4}	K_2CO_3	28	36	64
3	L_{P5}	K_2CO_3	28	36	64
4	L_{N1}	K_2CO_3	28	29	68
5	L_{N2}	K_2CO_3	28	36	64
6	L_{N3}	K_2CO_3	28	21	61
7	L_{N4}	K_2CO_3	28	39	61
8	L_{N5}	K_2CO_3	28	21	68
9	L_{P3}	KOH	28	33	64
10	L_{P3}	*t*-BuOK	25	28	72

*(0.025 mmol Ru complex, 1 mmol 1,6-HD, under N_2 atmosphere, 110 °C, 30 mL toluene, 0.2 mmol base, 8 mmol MIBK).

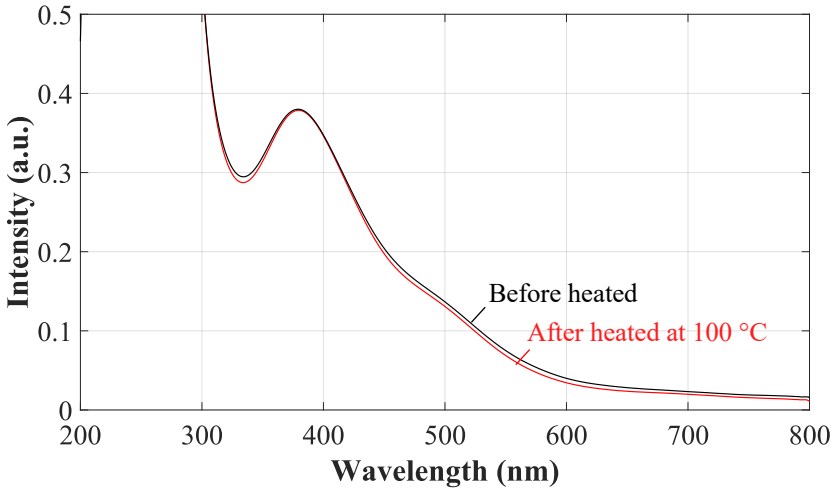

Figure S12. UV-VIS spectra of (*p*-cymene)$RuCl_2$(L_{P4}) a) before (–) and after (–) heated at 110 °C in the presence of K_2CO_3 in toluene.

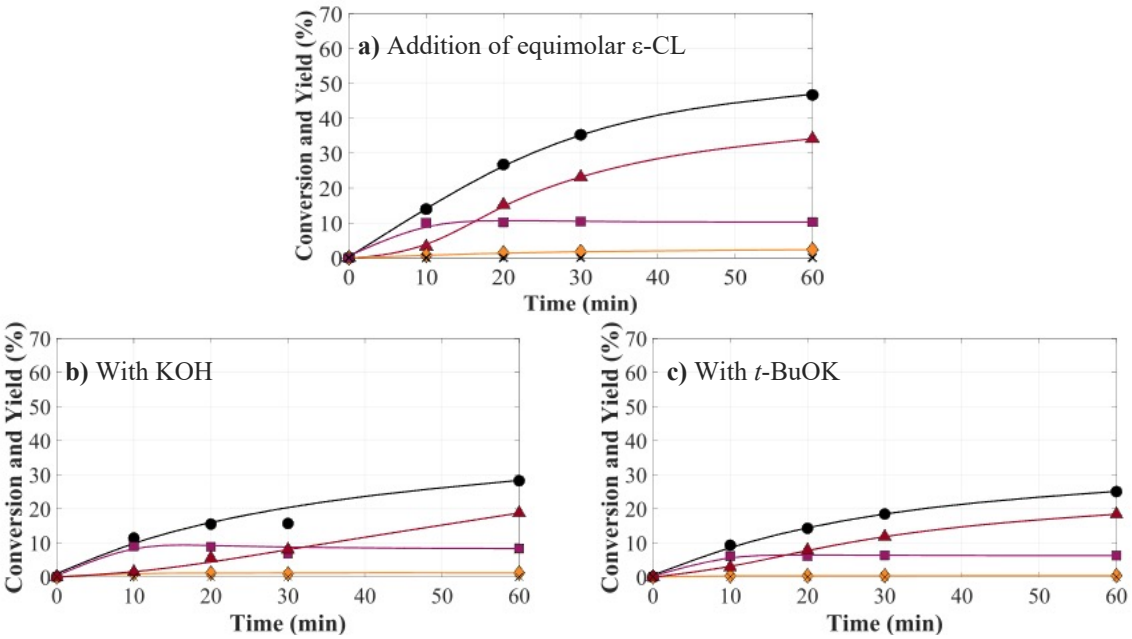

Figure S13. 1,6-HD oxidation time profile using (*p*-cymene)$RuCl_2(L_{P4})$ catalyst with a) the addition of equimolar ε-CL, b) KOH and c) *t*-BuOK (conversion (●), 6-hydroxyhexa-1-nal (■), 1,6-hexanedial (♦), ε-CL (▲), and adipic acid (✕) (0.025 mmol Ru complex, 1 mmol 1,6-HD, under N_2 atmosphere, 110 °C, 30 mL toluene, 0.2 mmol K_2CO_3, 8 mmol MIBK).

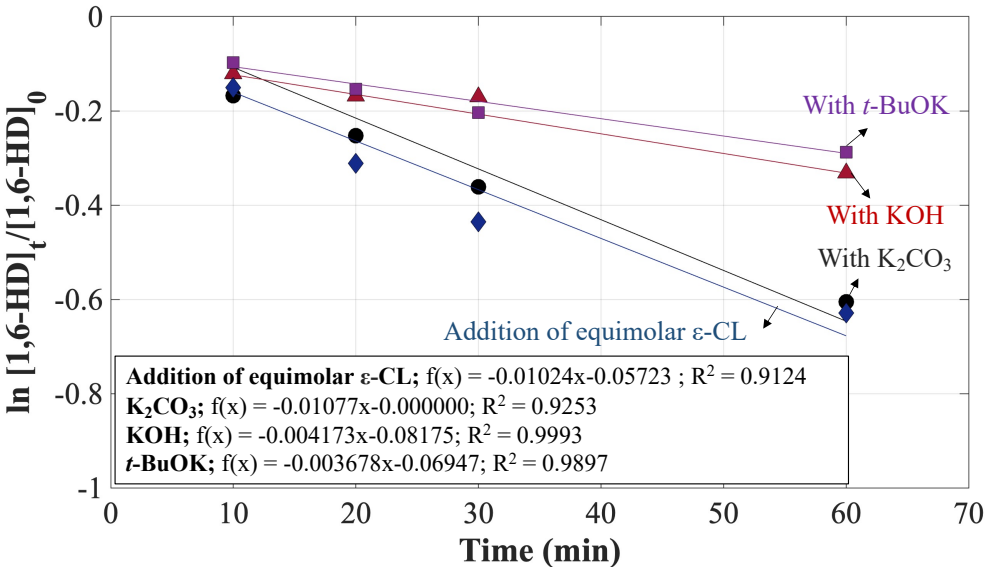

Figure S14. Kinetics plot of 1,6-HD oxidation using (*p*-cymene)$RuCl_2(L_{P4})$ catalyst with the addition of equimolar ε-CL (♦), K_2CO_3 (●), KOH (▲), and *t*-BuOK (■) (0.025 mmol Ru complex, 1 mmol 1,6-HD, under N_2 atmosphere, 110 °C, 30 mL toluene, 0.2 mmol base, 8 mmol MIBK).

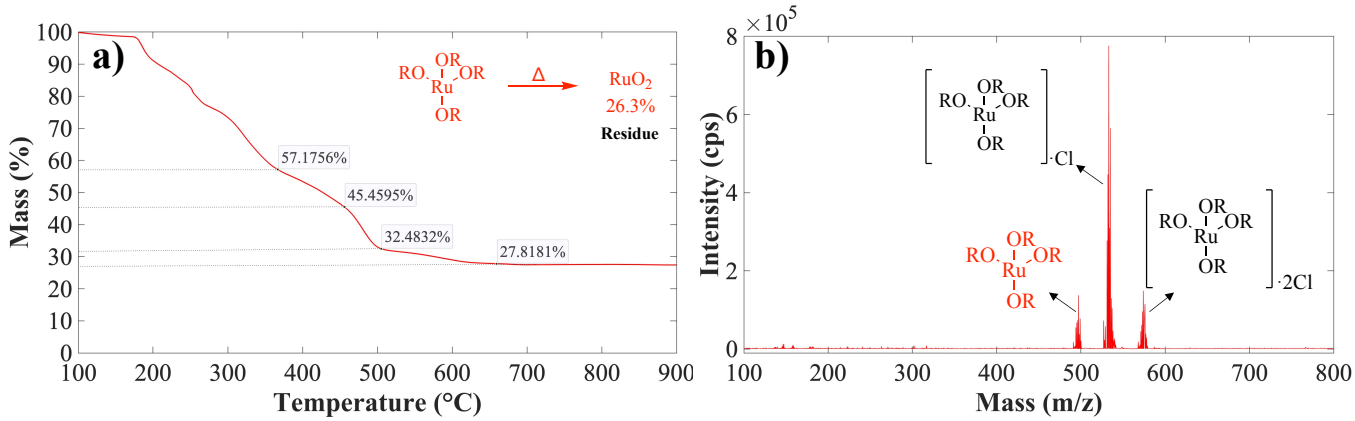

Figure S15. TGA curve under air-zero (a) and mass spectra (b) attained by QTOF mass spectrometry electrospray analysis of $Ru(MIBC)_4$, where OR is 4-methyl-2-pentanolate group.

In addition to ^{13}C CPMAS NMR (Figure 8), the TGA curve of the brown solids precipitated after mixing (*p*-cymene)$RuCl_2(L_{P4})$ and MIBC (in excess) showed a mass loss of ~72% of the decomposable organic fraction at 600 °C (Figure S15a). This can be attributed to four alkyl groups of MIBC, bearing approximately 28% of RuO_2 (134 g/mol) from the $Ru(MIBC)_4$ (506 g/mol). A slightly higher mass (~28%) compared to the theoretical value (~26%, 134×100/506) indicates a trace of Cl remained in the solid precipitate. This can be evidenced by QTOF mass spectra (Figure 15b), showing that M+35/37 ($Ru(MIBC)_4$·Cl, m/z~541/543) and M+70/74 ($Ru(MIBC)_4$·2Cl, m/z~576/578) are largely pronounced.

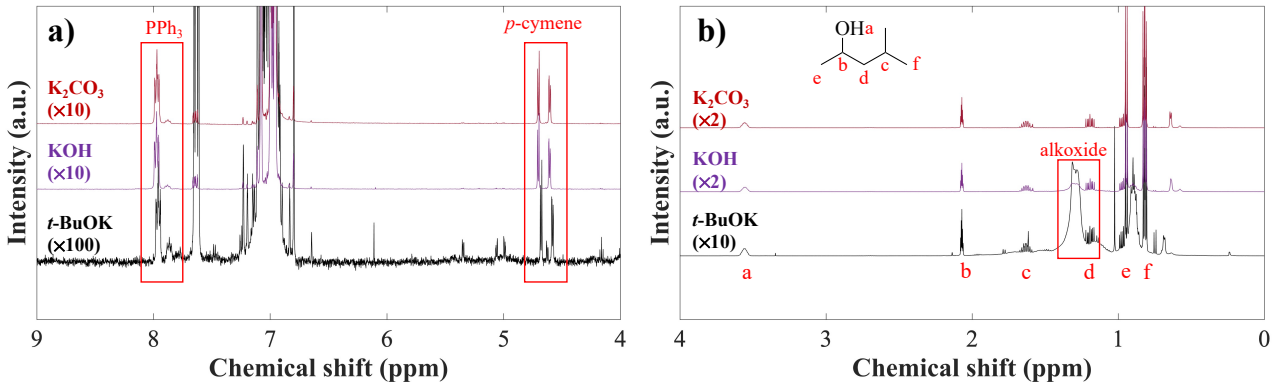

Figure S16. 500 MHz ^{1}H NMR spectra of the reaction of (*p*-cymene)$RuCl_2(L_{P4})$ with 34 mmol MIBC at 110 °C for 5 min in toluene-d_8 after left overnight; a) 0-10 ppm and b) zoom 0-4 ppm.

References

1 E. Solari, S. Gauthier, R. Scopelliti, K. Severin, *Organometallics,* 2009, **28**, 4519–4526.

2 E. Hodson, S. J. Simpson, *Polyhedron,* 2004, **23**, 2695–2707.

3 D. K. Gupta, A. N. Sahay, D. S. Pandey, N. K. Jha, P. Sharma, G. Espinosa, A. Cabrera, M. C. Puerta, P. Valerga, *J. Organomet. Chem.,* 1998, **568**, 23-20.

4 P. Chuklin, V. Chalermpanaphan, T. Nhukeaw, S. Saithong, K. Chainok, S. Phongpaichit, A. Ratanaphan, N. Leesakul, *J. Organomet. Chem,* 2017, **846**, 242–250.

5 H. Cao, L.-H. Cai, C.-X. Wang, X.-H. Zhu, Z.-M. Li, X.-F. Hou, *J. Organomet. Chem,* 2015, **775**, 60–66.

6 J. G. Małecki, M. Jaworska, R. Kruszynski, *Polyhedron,* 2006, **25**, 2519–2524.

7 A. Rodríguez-Bárzano, J. D. A. Fonseca, A. J. Blacker, P. C. McGowan, *Eur. J. Inorg. Chem.* 2014, **2014**, 1974–1983.